Zebrafish Hagoromo mutants upregulate fgf8 post-embryonically and develop neuroblastoma

Citation: Amsterdam, A. et al. "Zebrafish Hagoromo Mutants Up-Regulate Fgf8 Postembryonically and Develop Neuroblastoma." Molecular Cancer Research 7.6 (2009): 841–850.

As Published: http://dx.doi.org/10.1158/1541-7786.mcr-08-0555

Publisher: American Association for Cancer Research

Persistent URL: http://hdl.handle.net/1721.1/73548

Version: Author's final manuscript: final author's manuscript post peer review, without publisher's formatting or copy editing

Published in final edited form as:
Mol Cancer Res. 2009 June ; 7(6): 841–850. doi:10.1158/1541-7786.MCR-08-0555.

Zebrafish *Hagoromo* mutants upregulate *fgf8* post-embryonically and develop neuroblastoma

Adam Amsterdam[1], **Kevin Lai**[1], **Anna Z Komisarczuk**[2], **Thomas S Becker**[2,4], **Roderick T. Bronson**[3], **Nancy Hopkins**[1], and **Jacqueline A Lees**[1,5]

[1]David H. Koch Institute for Integrative Cancer Research @ MIT, Cambridge, MA 02139

[2]Sars Centre for Marine Molecular Biology, University of Bergen, Bergen, Norway

[3]Tufts Cummings School of Veterinary Medicine, North Grafton, MA 01536

Abstract

We screened an existing collection of zebrafish insertional mutants for cancer susceptibility by histological examination of heterozygotes at two years of age. As most mutants had no altered cancer predisposition, this provided the first comprehensive description of spontaneous tumor spectrum and frequency in adult zebrafish. Moreover, the screen identified four lines, each carrying a different dominant mutant allele of *Hagoromo* previously linked to adult pigmentation defects, which develop tumors with high penetrance that histologically resemble neuroblastoma. These tumors are clearly neural in origin, although they do not express catecholaminergic neuronal markers characteristic of human neuroblastoma. The zebrafish tumors result from inappropriate maintenance of a cell population within the cranial ganglia that are likely neural precursors. These neoplasias typically remain small but they can become highly aggressive, initially traveling along cranial nerves, and ultimately filling the head. The developmental origin of these tumors is highly reminiscent of human neuroblastoma. The four mutant *Hagoromo* alleles all contain viral insertions in the *fbxw4* gene, which encodes an F-box WD40 domain containing protein. However, while one allele clearly reduced the levels of *fbxw4* mRNA, the other three insertions have no detectable effect on *fbw4* expression. Instead, we show that all four mutations result in the post-embryonic upregulation of the neighboring gene, *fibroblast growth factor 8 (fgf8)*. Moreover, *fgf8* is highly expressed in the tumorigenic lesions. While *fgf8* overexpression is known to be associated with breast and prostate cancer in mammals, this study provides the first evidence that *fgf8* misregulation can lead to neural tumors.

Keywords

neural precursors; retrovirus; insertional mutagenesis; cancer

INTRODUCTION

The zebrafish is an increasingly popular model organism in which to study cancer (1). Mutation of known tumor suppressors such as nf2, p53, apc, and mlh1 (2-5) result in cancer susceptibility, and tumorigenesis can also be driven by the expression of a number of oncogenes such as c-myc (6), mutant Kras (7) or mutant braf (8). Additionally, forward genetic screens in zebrafish can identify novel mutations that lead to cancer susceptibility. For example, by screening initially for mutations that affect the cell cycle in homozygous embryos, mutations in bmyb

[5]Corresponding author: jalees@mit.edu, Tel: (617) 252 1972; Fax: (617) 253 9863.
[4]Current address: Brain and Mind Research Institute, University of Sydney, Camperdown NSW 2050, Australia

and separase were found to modestly increase the rate of carcinogen-induced cancer in heterozygous adults (9,10). In another study, by conducting a pilot screen of an existing collection of heterozygous carriers of embryonic lethal insertional mutations for the development of externally visible spontaneous tumors, we established that haploinsufficiency of 17 different ribosomal protein genes is highly tumorigenic (2,11). This validates the use of zebrafish to identify novel cancer genes.

The mutant collection used for this pilot screen includes over 500 mutations in over 370 genes (12). These mutations were made by retroviral insertion, allowing rapid identification of the mutated gene in almost all cases by cloning the genomic DNA flanking the mutagenic insertion (13). These mutants were recovered in a large-scale screen designed to find recessive mutations with embryonic phenotypes (14) and nearly all of the mutants are embryonic or larval lethal in their homozygous state. In the course of the screen we also recovered a few dominant mutations with viable adult phenotypes affecting either pigmentation or fin growth. None of these dominant mutations had any visible phenotypes during embryogenesis as either heterozygotes or homozygotes.

We maintain all of the zebrafish mutant lines as stocks of 15−25 heterozygotes until two years of age, thereby allowing for an assessment of adult phenotypes in the heterozygous state. In this study, we have extended our analysis of the full mutant collection by screening for spontaneous tumor development by histological examination as opposed to just externally visible tumors. This revealed that all four alleles of the dominant mutation *Hagoromo* (14, 15) were highly predisposed to the development of neuroblastoma-like tumors arising in the cranial ganglia.

RESULTS

Cancer screen of insertional mutants identifies *Hagoromo*

We had previously discovered that heterozygous mutation of many ribosomal protein (*rp*) genes, as well as the *nf2a* gene (one of two paralogs of the mammalian tumor suppressor NF2) predisposed zebrafish to the development of cancer, primarily malignant peripheral nerve sheath tumors (2). Notably, these mutants develop tumors spontaneously, in the absence of chemical carcinogens. While the ribosomal protein mutants generally developed large, externally visible tumors, the *nf2a* heterozygotes usually developed much smaller tumors that were only evident upon histological examination of the fish. Thus it is unlikely that we would have discovered that these fish were tumor-prone had we not examined sections of a cohort of apparently healthy fish. Reasoning that there might be other mutations which similarly predisposed fish to tumors that might not be externally visible, we set about to systematically examine heterozygotes from all of the insertional mutant lines in our collection by histology. Initially we examined at least fifteen fish for each line at approximately two years of age. In most cases two longitudinal sections near either side of the midline were examined, although in some cases six sections were screened. For any families that had a tumor frequency in the first cohort greater than background (see below), we collected additional two-year-old fish to determine if this was a true tumor predisposition or just a sampling artifact.

All of the analyzed fish, with the exception of those from lines that we determined to be tumor-prone, served as a control set. Analysis of these 10,000 fish from 437 lines (including mutations in 341 different genes) indicated that the “background” frequency of tumorigenic lesions, including pre-adenoma bile-duct hyperplasia, was about 5% at two years of age (473/9988). The most common tumor types were seminomas and bile duct lesions (hyperplasia, adenoma, and adenocarcinoma), followed by pancreatic islet cell adenoma and leukemia/lymphoma (Figure 1). None of these tumor types appeared in greater than 2% of the fish and we did not find any families in which these tumors were significantly overrepresented. As far as we are

aware, this is the first comprehensive analysis of spontaneous tumor incidence and spectrum in zebrafish.

Of the 342 loci screened in this manner, 339 were recessive embryonic lethal mutations. Beyond the previously noted *rp* and *nf2a* genes, none of the heterozygous carriers of recessive lethal mutations had a spontaneous cancer frequency significantly above background. This included mutations in two genes, c-myb and separase, whose heterozygous mutation has been shown to increase cancer frequency in carcinogen-treated fish (9,10). In addition to these recessive mutations, the collection contains dominant mutations in three loci that have no embryonic phenotype (as homozygotes or heterozygotes) but rather have viable visible adult phenotypes either in fin growth or stripe patterning. One of these loci, for which we have four mutant alleles, is *Hagoromo* (*Hag*). *Hag* mutants, named for "the dress of a goddess", are characterized by disorganized stripes in the adult pigment pattern that are first apparent during the reorganization of iridophores and melanophores during metamorphosis at 3−4 weeks of age (15). Neither heterozygotes nor homozygotes have any embryonic phenotype; homozygotes are viable and have, on average, more severe stripe defects than heterozygotes, sometimes resulting in a spotty appearance in the anterior flank. All four *Hag* alleles carry insertions in the *fbxw4* gene, which encodes an F-box containing WD-40 repeat protein (15). Our screen revealed a significant tumor predisposition in these four *Hag* alleles. In each of these lines, 25−50% of two-year-old heterozygotes had tumors that histologically resembled neuroblastoma (Table 1, Figure 2). Importantly, these neuroblastoma-like tumors were not observed in any of the ~10,000 screened fish that lacked insertions in the *fbxw4* gene, including 150 non-carrier siblings from the *Hag* families. Thus, we conclude that fish without insertions in the *Hag* locus spontaneously develop this tumor type with a frequency less than 1/10,000. This, coupled with the observation that four different insertions in this locus lead to this tumor type, indicates that the insertions at the *Hag* locus are unquestionably responsible for these cancers.

Hagoromo tumors resemble neuroblastoma and are preceded by the inappropriate maintenance of a putative neural precursor cell population

To better understand the nature and origin of these tumors, we conducted a careful analysis of the *Hag* fish. Hematoxylin and eosin staining indicated that the tumors in *Hag* fish indicated that the tumors were made up of small, densely packed, oval cells with very little cytoplasm (Figure 2). While in some tumors, cells were arranged in "rosettes" (Figure 2B) commonly seen in partly differentiated human neuroblastoma (16), more frequently the cells were simply present as sheets with little organization (Figure 2C) as is seen in undifferentiated human neuroblastoma (16). The tumors were found in a wide range of sizes, from small neoplasias (20−30 cells per planar section) to large tumors that occupied nearly the entire head, pushing aside (though never invading) the brain and pushing into musculature of the cheeks and dorsal body wall. The highly aggressive tumors, such as that shown in Figure 2A, were least common, and we rarely observed fish with any external signs of tumor growth, such as a bump on the dorsal surface or bulging of an eye. Small neoplasias were most common (Table 1) and always arose in cranial ganglia, either just below the midbrain but still within the skull (Figure 2D) or in ganglia projecting posteriorly from behind the ear (Figure 2E). As these tumors grew larger, they clearly overtook the entire ganglia and tracked along nerves, for example those leaving the skull and projecting towards the ear or behind the eye (Figure 2F). These tumors did not appear to be ganglioneuromas as they did not produce ganglion cells as they grew. Thus, based upon the origin of these tumors in ganglia as well as their histological appearance, we suspected that they were neuroblastomas. By staining with the pan-neural marker HuC we confirmed that these tumors were of neural origin (Figure 2G-H). However, the tumors failed to stain for tyrosine hydroxylase (Figure 2I). This marker is expressed in the catecholaminergic neurons of the peripheral sympathetic nervous system that are most often the cell of origin for human

neuroblastoma (17,18). So while these tumors were unquestionably neural and histologically resemble human neuroblastoma, they did not appear to arise from the same population of neurons that contributes to most human neuroblastoma. However, they may share other characteristics with the human disease.

Neuroblastoma is usually a neonatal or childhood cancer in humans. Tumors of this class typically orginate from a precursor/progenitor population that persists inappropriately because of a failure to instigate the normal differentiation and/or apoptotic program (18,19). In order to determine the origin of the tumors in *Hag* zebrafish, we conducted a time course analysis of the progeny of *Hag* heterozygous crosses (including wild type, heterozygous, and homozygous sibs) by analyzing a subset of each cohort at one-month intervals. The cranial ganglia of one-month-old fish contained clusters of cells that appeared very similar in size, shape, and organization to the tumor cells (Figure 3A-B). These were found in both wild type and mutant fish, and thus we conclude that this is a normal developmental stage. However, by two months of age, these cells appeared less frequently and are fewer in number in wild type fish than in either heterozygous or homozygous *Hag* fish (data not shown). This was even more apparent at three months, by which time these cells were completely absent in the wild type fish, but they were maintained within almost all of the heterozygous and homozygous *Hag* mutants (Figure 3C-D, Table 2). These cells were neural as they strongly express HuC (Figure 3E-H). Taken together, these data suggest that the presence of this cell population in the wild type zebrafish denotes a stage of neuronal development that is normally completed before 3 months of age. The simplest explanation of this finding is that these cells represent a neural precursor population. We believe that the persistence of these cells in 3 month old *Hag* mutants is an early event in the tumorigenic process. Notably, these small neoplasias occurred at a similar frequency in both heterozygous and homozygous *Hag* mutants.

By as early as 5 months these neoplasias began to grow into advanced tumors in a small proportion of *Hag* fish, spreading throughout entire ganglia and following nerve bundles away from their site of origin (Fig 3I-J). These advanced tumors emerged at a slightly higher rate in homozygotes than in heterozygotes (Table 2). However, our ability to track the tumor development in homozygotes was compromised by an additional phenotype of the homozygous fish; with variable penetrance they develop severe inflammation in the wall of the posterior esophagus and anterior gut, leading to wasting and eventual mortality, possibly due to starvation (Table 2, Figure S1). Taken as a whole, this time course experiment indicates that heterozygotes and homozygotes have a similar propensity to inappropriately maintain this presumed precursor cell population but these neoplasias develop into more advanced tumors at a somewhat faster rate in homozygous versus heterozygous *Hag* mutants.

Hag mutations upregulate *fgf8* expression rather than affect *fbxw4*

We wished to determine how the *Hag* mutant alleles contribute to the tumorigenic state. The insertional mutants used in this screen were made with Moloney Murine Leukemia Virus (MoMLV)-based vectors. In mammals, MoMLV insertions can cause either gene activation through enhancer activity of the viral LTRs or inactivation by disruption of splicing or coding sequences (20,21). Most of the mutants we recovered in our screen were recessive (491/497), and we isolated only six dominant mutations that represent insertions in three different loci (12,14, A.A. and N.H. unpublished data). Molecular analysis demonstrates that in all of the recessive mutations that we have examined, expression of the gene in which the insertion lies is reduced or abrogated (11,13,22, A.A. and N.H. unpublished data). In contrast, the cause of the dominant mutations is less clear; they could be loss-of-function alleles of haploinsufficient loci or gain-of-function alleles.

To understand why the *Hag* mutants are tumor-prone, we first examined if expression of the *fbxw4* gene was affected, as all of the insertions lie within this gene, hiD2058 at the splice

donor of the first exon and hiD1, hiD2 and hiD4000 all in the fifth intron (Figure 4A). We chose to analyze gene expression in homozygotes as this would facilitate the detection of gene expression changes in cis to the insertion, especially if the effect was down-regulation. We used real time reverse transcriptase polymerase chain reaction (RTPCR) on RNA isolated from whole fish. We examined expression of *fbxw4* in wild type fish and homozygotes for three of the lines at two developmental stages: the end of embryogenesis (5 days) and after juvenile morphogenesis (6 weeks), when the pigment phenotype that is the defining characteristic of the *Hag* mutants is clearly visible (Figure 4B). For hiD2058, the mutant with an insertion at the splice donor of the first exon, expression was reduced to approximately 1% of wild type levels (Figure 4B). Additional analysis indicated that this insertion interferes with the splicing of the message, utilizing a cryptic splice site in the first exon upstream of the initiation codon (data not shown). Thus for hiD2058, the level of *fbxw4* is greatly reduced and also incapable of producing full-length protein, if any protein at all. However, for two of the lines with insertions in the fifth intron (hiD1 and hiD4000), there was no change in level of fbxw4 mRNA at either of these time points (Figure 4B). Since all of the alleles have the same phenotype (both pigment and tumor phenotypes) but at least two of the three alleles with insertions in the large intron do not affect fbxw4 expression (expression in hiD2 was not examined), it is unlikely that the loss of *fbxw4*, even in hiD2058, is responsible for any of the observed phenotypes.

The gene immediately upstream of *fbxw4* is *fgf8* (Figure 4A), and this juxtaposition is conserved between fish and mammals. *Fgf8* is a common site for mouse mammary tumor virus (MMTV) insertions in murine mammary cancer, where viral insertions lead to *fgf8* overexpression (23-25). There are even some reported cases where MMTV had inserted in the murine *fbxw4* gene to cause activation of *fgf8* (25). Although we have not previously seen the MoMLV virus activate genes in zebrafish, given the mouse results we thought it would be prudent to examine the effects of these insertions upon *fgf8* expression in a manner identical to that used for *fbxw4*. During embryogenesis, *fgf8* expression is very dynamic and its function is especially important, as both loss-of-function mutants and mutations that lead to *fgf8* overexpression have early embryonic phenotypes (26,27). In wild type fish, *fgf8* expression declines after embryogenesis (Figure 4C) though it is known to remain expressed in some tissues (28,29). During embryogenesis, we did not see any difference in *fgf8* mRNA levels between whole wild type fish and *Hag* homozygotes (Figure 4C). However, at six weeks of age, *fgf8* mRNA levels were 6−12 times higher in *Hag* homozygotes than in wild type controls for all three lines tested (Figure 4B). To further explore this deregulation, we examined *fgf8* mRNA levels in wild type and homozygous fish over a number of intervening time points for one allele (hiD4000, Figure 4C). In wild type fish, the overall level of *fgf8* mRNA began to decline 1−2 weeks after embryogenesis was complete and *fgf8* mRNA dropped to very low levels by 5−6 weeks of age. In contrast, the amount of *fgf8* mRNA was maintained at near-embryonic levels in *Hag* homozygotes throughout the time course. Notably, there is an excellent correlation between the loss or maintenance of *fgf8* mRNA in the wildtype and *Hag* mutant fish and the loss or maintenance of the presumed neural precursor population. Importantly, the timeframe of *fgf8* downregulation precedes the loss of the putative precursor cells in wild type fish suggesting that high *fgf8* somehow contributes to the maintenance of this population in the *Hag* mutants. As expression was measured from RNA prepared from whole fish, it is not clear if this difference is the result of higher levels of *fgf8* in cells that normally express it or ectopic expression of *fgf8*. Nonetheless, it is clear that *fgf8* is dramatically upregulated in *Hag* mutants and that it is likely *fgf8*, not *fbxw4*, which is the gene responsible for the *Hagoromo* phenotypes. Consistent with this hypothesis, we note that an enhancer trap screen using another MoMLV-based retrovirus (30) has yielded two insertions, CLGY1030 and CLGY508 (31), that lie in intergenic sequences upstream and downstream of *fgf8*, respectively (fig 4A). Analysis of *fgf8* expression in these mutants revealed both increased *fgf8* expression in the midbrain-hindbrain boundary at 3 dpf and ectopic *fgf8* expression in the spinal region of 35 dpf fish, and these two mutants develop a stripe phenotype that is highly

reminiscent of our *Hagoromo* mutants (A.Z.K and T.S.B., unpublished data). Histological analysis of these lines show that they also develop neuroblastoma tumors (Figure S2). Taken together, these data strongly suggest that the tumor predisposition in these six lines result from a failure to downregulate *fgf8* subsequent to embryogenesis and the consequent persistence of a putative neuronal precursor population.

As a further test of this hypothesis, we wished to determine if increased *fgf8* expression occurs in the region of the cranial ganglia where the tumors originate. Thus we analyzed *fgf8* expression by both semi-quantitative RT-PCR and real-time RT-PCR on mRNA from several parts of the head of wild type and both heterozygous and homozygous *Hag* fish at 3 months of age, the time at which the clusters of neural precursors are first completely absent in wild type fish but maintained in the *Hag* mutants. The tissues analyzed included the brain, the skull, the soft tissue ventral to the skull (which included the cranial ganglia), and the jaws and skin. Of these tissues, the brain had the highest overall *fgf8* expression in wild type fish, and *fgf8* expression appeared slightly higher in the brain of *Hag* mutants. The other three tissues, where *fgf8* was expressed at a low level in wild type fish, showed dramatically higher levels of *fgf8* in *Hag* mutants (Figure 5A). Thus, we conclude that elevated *fgf8* expression is not restricted to the cranial ganglia but is clearly present in this region of the *Hag* mutants. Most importantly, *in situ* hybridization with antisense *fgf8* probe on sections cut from fish with tumors shows robust expression of *fgf8* in most, although not all, cells in the tumor (Figure 5B-C). Thus, we conclude that the neuroblastomas themselves express *fgf8* at a very high level.

DISCUSSION

Through the unbiased histological screening of a collection of zebrafish insertional mutants, we determined that four independent lines carrying mutations in the *Hagoromo* locus develop neuroblastoma-like tumors at high penetrance. In some regards, these tumors are quite different than human neuroblastoma, which arises from neural crest-derived neural precursors in the sympathetic nervous system and grow predominantly in the abdomen or neck (17,18). Tumors in *Hagoromo* fish arise in cranial ganglia and grow in the head. While they are clearly of neural origin, as judged by their expression of HuC, these zebrafish tumors do not express markers of catecholaminergic neurons indicating that they are derived from a different neural lineage than human neuroblastoma. Despite this difference, the *Hagoromo* tumors seem to arise through a similar mechanism as the human disease. Specifically, human neuroblastoma typically arises in infants and is thought to be a tumor of embryonic origin, i.e. derived from neural precursors present during fetal development (18,19). Our analysis shows that wildtype zebrafish have a population of cells which exists in the cranial ganglia of juvenile fish but is lost as the fish grow to adulthood. We hypothesize that these cells represent neural precursors and their disappearance, presumably through differentiation or apoptosis, reflects the normal developmental program. These cells are inappropriately maintained in *Hagoromo* mutants and they are the originating cell of the *Hagoromo* mutant tumors. While in many cases these clusters of cells fail to grow past the size of small neoplasias, in 10−20% of the mutants they eventually grow into advanced tumors beginning as early as five months. This stochastic event likely reflects the need to acquire additional mutations within these cells. The *Hagoromo* mutation seems to act by prolonging the existence of, and possibly driving the expansion of, this target cell population.

The four *Hagoromo* mutant lines each carry viral insertions in the *fbxw4* gene. However, our data show that they do not have a shared effect on *fbxw4* expression: one allele, in which the insertion lies at the splice donor of the first exon, does diminish *fbxw4* mRNA levels, but the other insertions, which lie in the fifth intron, have no detectable effect on *fbxw4*. Instead, our data suggest that the key consequence of the *Hagoromo* insertions is to maintain high levels of *fgf8* expression after embryogenesis. Specifically, we find that *fgf8* mRNA is dramatically

upregulated in *Hagoromo* mutants after the completion of embryonic development, including expression in the head region where the inappropriately maintained precursors are first observed. In addition, very high *fgf8* expression is seen in the tumors themselves. Finally, insertional mutants have been recovered with a related virus from a different screen with phenotypes including both the stripe phenotype and the neuroblastoma phenotype in which the insertions lay outside of *fbxw4*, either between *fgf8* and *fbxw4* or upstream of *fgf8*, distal to *fbxw4*.

The mechanism by which these insertions activate *fgf8* expression is unclear. That the gene containing the viral insertions is not truly the affected gene should serve as a cautionary example for the analysis of other insertional mutants. In this case, although we cannot rule out direct viral activation, our previous studies suggest that the MoMLV LTR does not activate transcription in zebrafish cells; viruses relying upon the LTR to drive expression of the *lacZ* gene produced no ß-galactosidase activity while viruses with an internal promoter driving *lacZ* were able to do so (32). Additionally, in all other cases where the expression of genes at the site of MoMLV insertions in zebrafish has been examined, gene expression has either decreased or been unaffected (11,13,22,33). Thus, we instead favor the notion that the virus disrupts the transcriptional control of *fgf8* by distal *cis*-acting elements. This hypothesis is supported by several lines of evidence showing that *fgf8* expression is controlled by a number of enhancers upstream, within, and downstream of the gene, including elements within the *fbxw4* gene (31,34,35). Additionally, retroviral insertions in the *Fgf8/Fbxw4* locus in the mouse (36-37) or genomic duplications near *FGF8* in humans (38-39) cause a limb outgrowth phenotype (dactylaplasia or split hand foot malformation). The mechanism of these mouse and human mutations is not understood. However, the mouse mutants have been shown to have a defect in the maintenance of the apical ectodermal ridge (AER) of the developing limb, and *Fgf8* expression is normal at the beginning of limb development but is quickly lost (36). While it has been suggested that this altered *Fgf8* expression is a secondary consequence of AER loss, it also seems possible that the insertions in the mouse dactylaplasia mutants affect *fgf8* expression in a direct, but complex, way that somehow accounts for the observed downregulation after limb development begins. Although the molecular and phenotypic consequences of insertions and chromosomal rearrangements of the *Fgf8/Fbxw4* locus clearly differ between mammals and fish, it seems plausible that the resulting phenotypes in each organism (limb outgrowth defects in mammals, maintenance of neural precursor cells and stripe disruption in zebrafish) can be accounted for by differential effects upon *fgf8* expression.

Regardless of the mechanism by which the zebrafish insertions cause continued high levels of *fgf8* expression after embryogenesis, it clearly leads to the inappropriate maintenance and expansion of a putative neural precursor population that ultimately become tumors. We note that the increase in *fgf8* expression in the head region of *Hagoromo* fish occurs at a time when this cell population diminishes in wild type fish. This suggests that *fgf8* is capable of contributing to the maintenance of these cells, either by blocking differentiation or promoting survival. It would seem paradoxical that *fgf8* should prevent differentiation of these precursor cells as many studies have associated *fgf8* with neural differentiation. A requirement for *fgf8* in the development of neurons in various areas of both the central and peripheral nervous system, including the epibranchial placodes that give rise to the cranial ganglia, has been demonstrated both in zebrafish, (40-42) and in mice (43). Furthermore, *Fgf8* cooperates with retinoic acid to force mouse embryonic carcinoma P19 cells to differentiate into neurons while inhibition of fgf signaling in this cell culture system attenuates neural differentiation (44). However, this pro-differentiation role for *fgf8* might be restricted to specific developmental stages such as embryogenesis. For example, in some settings *fgf8* signaling can promote proliferation of neural precursors at the expense of differentiation (45). The other possibility, that *fgf8* acts as a pro-survival signal for these cells, is supported by the observation that several fgfs, including *fgf8*, have anti-apoptotic functions in both neural crest and ectoderm-derived

neurons (43,46). The effects of *fgf8* upon differentiation and survival may depend upon timing and context, such that early in development neural differentiation is the favored response, but sustained *fgf8* expression past the time when such differentiation normally occurs may result in inappropriate survival and/or proliferation of the few remaining neural precursor cells.

Thus *fgf8* appears to be an oncogene, in that its overexpression predisposes zebrafish to tumorigenesis. However, the tumor phenotype in *Hagoromo* mutants is not fully penetrant. Notably, it appears that *fgf8* overexpression in *Hagoromo* mutants is always sufficient to disrupt the orderly alignment of pigment cells (which are moving into their stripe pattern at the time when we first see *fgf8* overexpression in the mutants), as well as the inappropriate maintenance of putative neural precursor cells in cranial ganglia. However, these only progress to tumors in a subset of cases, suggesting that additional mutations are required. It is possible that there is only a limited window of opportunity for the precursor cell population to acquire these changes. This model is supported by our finding that small neoplasias exist in nearly all of the mutants at 3−6 months of age (and we might miss some due to sampling only three sections per fish) but are detected in fewer than half of the fish at two years of age. Thus, we speculate that *fgf8* overexpression allows for the persistence of a cell population that is then a target for additional mutations, and there may be a limited time in which such mutations can contribute to tumorigenesis. We do not currently know what these additional mutagenic events are, and this is an important question for future study. However, we believe it is unlikely that mutation of the tumor suppressor gene *p53* is one such key event, as fish mutant for both *Hagoromo* and *p53* (3) do not have a higher rate of neuroblastoma formation by one year of age than fish mutant for *Hagoromo* alone (data not shown).

Fgf8 has also been implicated in tumorigenesis in other tumor types in mammals. Overexpression of *FGF8* has been observed in a number of human tumors, especially prostate and breast cancer (47-49). Furthermore, whole genome association studies indicate that specific polymorphisms in the fgf receptor *FGFR2* correlate with an increased frequency of breast cancer (50,51). Direct evidence for the oncogenic properties of *Fgf8* in these tissues is even clearer in mice. The *Fgf8* locus is a common insertion site for MMTV in retrovirus-induced mammary tumors (23-25), implying that its activation in mammary tissue can lead to tumorigenesis. Additionally, transgenic tissue-specific overexpression of *Fgf8* cooperates with *Pten* loss in mouse models of prostate cancer (52). Thus, *FGF8* appears to function as oncogene in numerous settings including prostate and breast cancer in mammals, and now neuroblastoma in zebrafish.

MATERIALS AND METHODS

Fixation and Histology

Adult fish were euthanized in 500mg/L Tricaine and fixed in either Bouin's fixative or 10% neutral buffered formalin (in cases where we wished to retain the option of immunohistochemistry or in situ hybridization). Embedding in paraffin and sectioning were performed as previously described (2,53). Prior to fixation a piece of tail tissue was retained for the isolation of genomic DNA and either Southern analysis or PCR was conducted to determine the genotype of fish from the *Hag* heterozygous crosses (54).

Antibody staining

Slides from fish fixed in 4% paraformaldehyde/PBS and paraffin embedded were stained as previously described (55). Primary antibodies used were anti-TH (P40101−0, 1:100, Pel-Freez, Rogers AR) and anti-HuC (16A11, 1:250, Molecular Probes, Eugene OR)

RNA In Situ Hybridization

Dig-labeled riboprobes were produced for both sense and antisense strands of the coding regions of the zebrafish *fgf8* and *HuC* genes using a dig-labeling kit (Roche 11175033910) Slides from fish fixed in 4% paraformaldehyde/PBS and paraffin embedded were dewaxed (55), rinsed with PBS, treated with Proteinase K (40 μg/ml) for 7 min, rinsed with PBS, refixed in 4% paraformaldehyde/PBS for 20 min, rinsed with PBS, andrinsed twice in 2X SSC. They were then prehybridized in hybridization solution (50% formamide, 5X SSC, 0.1% Tween, 1 mg/ml tRNA, 50 μg/ml heparin) for 3 hours at 70°C, and hybridized overnight at 70°C in a humid box with 100 μl hybridization solution plus probe (1 μg/ml) under a cover slip. Slides were washed at 70°C for 10 min with 75% hyb/25% 2X SSC, 50% hyb/50% 2X SSC, 25% hyb/75% 2X SSC, 2X SSC, and for 30 min with 0.2X SSC. Slides were equilibrated in MAB + 0.1% tween for 30 min, blocked MAB + 0.1% tween + 10% lamb serum + 2% blocking reagent (Roche 11096176001) then AP-conjugated anti-DIG Fab fragments were applied (1:1000, Roche 11093274910) overnight at 4°C. Antibody was washed 5 × 30 min in MAB + 0.1% Tween, and AP activity was detected with NBT/BCIP as recommended by the maufacturer (Roche, 11383213001 and 11383221001). Figures show results with antisense probes; no blue stain was observed with sense-strand probes of simultaneously processed adjacent-level slides.

Quantitative RNA analysis

RNA was prepared from embryos, adult fish tissues, or whole juvenile fish using Trizol reagent (Invirtrogen, Carlsbad CA); in the case of whole fish 17dpf or older, fish were flash-frozen in liquid nitrogen and mashed in a mortar and pestle prior to homogeniztion in Trizol. First strand cDNA was prepared using Superscript III reverse transcriptase (Invirtrogen, Carlsbad CA) and gene expression levels were determined using real time PCR with Sybr Green Master Mix (ABI). Standard curves were established for each primer set with cDNA dilutions and all samples were run in triplicate and normalized with primers for gapdh. All primer sequences are available upon request.

Supplementary Material

Refer to Web version on PubMed Central for supplementary material.

ACKNOWLEDGEMENTS

We thank Sarah Farrington and Kate Anderson for maintenance of the mutant lines of fish and assistance in sample collection, and Tim Angelini and Sam Farrington for maintenance of the zebrafish colony. We thank the Histology Facility of the MIT Koch Institute for Integrative Cancer Research, especially Alicia Caron and Weijia Zhang, for sample processing and sectioning. We thank Drs. A. Thomas Look and Jeffery Kutok for helpful discussions and consultation on histopathology. N.H. and J.A.L. were funded by an NIH-NCI grant (CA106416). T.S.B. was supported by grants from the Sars Centre, the National Programme in Functional Genomics (FUGE) in Norway, and by the European Commission as part of the ZF-Models Integrated Project in the 6th Framework Programme (Contract No. LSHG-CT-2003−503496). J.A.L. is a Ludwig Scholar at MIT.

REFERENCES

1. Feitsma H, Cuppen E. Zebrafish as a Cancer Model. Mol Cancer Res 2008;6:685–94. [PubMed: 18505914]
2. Amsterdam A, Sadler KC, Lai K, et al. Many ribosomal protein genes are cancer genes in zebrafish. PLoS Biol 2004;2:E139. [PubMed: 15138505]
3. Berghmans S, et al. tp53 mutant zebrafish develop malignant peripheral nerve sheath tumors. Proc Natl Acad Sci U S A 2005;102:407–12. [PubMed: 15630097]
4. Haramis AP, Hurlstone A, van der Velden Y, et al. Adenomatous polyposis coli-deficient zebrafish are susceptible to digestive tract neoplasia. EMBO Rep 2006;7:444–9. [PubMed: 16439994]

5. Feitsma H, Kuiper RV, Korving J, Nijman IJ, Cuppen E. Zebrafish with mutations in mismatch repair genes develop neurofibromas and other tumors. Cancer Res 2008;68:5059–66. [PubMed: 18593904]
6. Langenau DM, Traver D, Ferrando AA, et al. Myc-induced T cell leukemia in transgenic zebrafish. Science 2003;299:887–90. [PubMed: 12574629]
7. Langenau DM, Keefe MD, Storer NY, et al. Effects of RAS on the genesis of embryonal rhabdomyosarcoma. Genes Dev 2007;21:1382–95. [PubMed: 17510286]
8. Patton EE, Widlund HR, Kutok JL, et al. BRAF mutations are sufficient to promote nevi formation and cooperate with p53 in the genesis of melanoma. Curr Biol 2005;15:249–54. [PubMed: 15694309]
9. Shepard JL, Amatruda JF, Stern HM, et al. A zebrafish bmyb mutation causes genome instability and increased cancer susceptibility. Proc Natl Acad Sci U S A 2005;102:13194–9. [PubMed: 16150706]
10. Shepard JL, Amatruda JF, Finkelstein D, et al. A mutation in separase causes genome instability and increased susceptibility to epithelial cancer. Genes Dev 2007;21:55–9. [PubMed: 17210788]
11. Lai K, Amsterdam A, Farrington S, et al. Many ribosomal protein mutations are associated with growth impairment and tumor predisposition in zebrafish. Dev Dyn. 2008in press
12. Amsterdam A, Nissen RM, Sun Z, et al. Identification of 315 genes essential for early zebrafish development. Proc Natl Acad Sci U S A 2004;101:12792–7. [PubMed: 15256591]
13. Gaiano N, Amsterdam A, Kawakami K, et al. Insertional mutagenesis and rapid cloning of essential genes in zebrafish. Nature 1996;383:829–32. [PubMed: 8893009]
14. Amsterdam A, Burgess S, Golling G, et al. A large-scale insertional mutagenesis screen in zebrafish. Genes Dev 1999;13:2713–24. [PubMed: 10541557]
15. Kawakami K, Amsterdam A, Shimoda N, et al. Proviral insertions in the zebrafish hagoromo gene, encoding an F-box/WD40-repeat protein, cause stripe pattern anomalies. Curr Biol 2000;10:463–6. [PubMed: 10801422]
16. Machin, GA. Histogenesis and histopathology of neuroblastoma.. In: Pochedly, C., editor. Neuroblastoma: Clinical and biological manifestations. Elsevier Biomedical; New York: 1982. p. 195-231.
17. McConville CM, Forsyth J. Neuroblastoma – a developmental perspective. Cancer Lett 2003;197:3–9. [PubMed: 12880953]
18. Brodeur, GM.; Maris, JM. Neuroblastoma.. In: Pizzo, PA.; Poplack, DG., editors. Principles and practice of pediatric oncology. Lippincott Williams & Wilkins; Philadelphia: 2002. p. 895-937.
19. Dyer MA. Mouse models of childhood cancer of the nervous system. J Clin Pathol 2004;57:561–76. [PubMed: 15166259]
20. Jaenisch R, Soriano P. Retroviruses as tools for mammalian development. Symp Fundam Cancer Res 1986;39:59–65. [PubMed: 3321310]
21. Mikkers H, Berns A. Retroviral insertional mutagenesis: tagging cancer pathways. Adv Cancer Res 2003;88:53–99. [PubMed: 12665053]
22. Golling G, Amsterdam A, Sun Z, et al. Insertional mutagenesis in zebrafish rapidly identifies genes essential for early vertebrate development. Nat Genet 2002;31:135–40. [PubMed: 12006978]
23. MacArthur CA, Shankar DB, Shackleford GM. Fgf-8, activated by proviral insertion, cooperates with the Wnt-1 transgene in murine mammary tumorigenesis. J Virol 1995;69:2501–07. [PubMed: 7884899]
24. Valve EM, Tasanen MJ, Ruohola JK, Harkonen PL. Activation of Fgf8 in S115 mouse mammary tumor cells is associated with genomic integration of mouse mammary tumor virus. Biochem Biophys Res Commun 1998;250:805–8. [PubMed: 9784427]
25. Theodorou V, Kimm MA, Boer M, et al. MMTV insertional mutagenesis identifies genes, gene families and pathways involved in mammary cancer. Nat Genet 2007;39:759–69. [PubMed: 17468756]
26. Reifers F, Bohli H, Walsh EC, Crossley PH, Stainier DY, Brand M. Fgf8 is mutated in zebrafish acerebellar (ace) mutants and is required for maintenance of midbrainhindbrain boundary development and somitogenesis. Development 1998;125:2381–95. [PubMed: 9609821]
27. Heisenberg C-P, Brennan C, Wilson SW. Zebrafish aussichtmutant embryos exhibit widespread overexpression of ace (fgf8) and coincident defects in CNS development. Development 1999;126:2129–2140. [PubMed: 10207138]

28. Albertson RC, Yelick PC. Fgf8 haploinsufficiency results in distinct craniofacial defects in adult zebrafish. Dev Biol 2007;306:505–15. [PubMed: 17448458]
29. Topp S, Stigloher C, Komisarczuk AZ, Adolf B, Becker TS, Bally-Cuif L. Fgf signaling in the zebrafish adult brain: association of Fgf activity with ventricular zones but not cell proliferation. J Comp Neurol 2008;510:422–39. [PubMed: 18666124]
30. Ellingsen S, Laplante MA, Konig M, et al. Large-scale enhancer detection in the zebrafish genome. Development 2005;132:3799–811. [PubMed: 16049110]
31. Kikuta H, Laplante M, Navratilova P, et al. Genomic regulatory blocks encompass multiple neighboring genes and maintain conserved synteny in vertebrates. Genome Res 2007;17:545–55. [PubMed: 17387144]
32. Gaiano N, Allende M, Amsterdam A, Kawakami K, Hopkins N. Highly efficient germ-line transmission of proviral insertions in zebrafish. Proc Natl Acad Sci U S A 1996;93:7777–82. [PubMed: 8755552]
33. Wang D, Jao LE, Zheng N, et al. Efficient genome-wide mutagenesis of zebrafish genes by retroviral insertions. Proc Natl Acad Sci USA 2007;104:12428–33. [PubMed: 17640903]
34. Inoue F, Nagayoshi S, Ota S, et al. Genomic organization, alternative splicing, and multiple regulatory regions of the zebrafish fgf8 gene. Dev Growth Differ 2006;48:447–62. [PubMed: 16961592]
35. Beermann F, Kaloulis K, Hofmann D, Murisier F, Bucher P, Trumpp A. Identification of evolutionarily conserved regulatory elements in the mouse Fgf8 locus. Genesis 2006;44:1–6. [PubMed: 16397882]
36. Sidow A, Bulotsky MS, Kerrebrock AW, et al. A novel member of the F-box/WD40 gene family, encoding dactylin, is disrupted in the mouse dactylaplasia mutant. Nat Genet 1999;23:104–7. [PubMed: 10471509]
37. Kano H, Kurahashi H, Toda T. Genetically regulated epigenetic transcriptional activation of retrotransposon insertion confers mouse dactylaplasia phenotype. Proc Natl Acad Sci U S A 2007;104:19034–19039. [PubMed: 17984064]
38. de Mollerat XJ, Gurrieri F, Morgan CT, et al. A genomic rearrangement resulting in a tandem duplication is associated with split hand-split foot malformation 3 (SHFM3) at 10q24. Hum Mol Genet 2003;12:1959–1971. [PubMed: 12913067]
39. Lyle R, Radhakrishna U, Blouin JL, et al. Split-hand/split-foot malformation 3 (SHFM3) at 10q24, development of rapid diagnostic methods and gene expression from the region. Am J Med Genet A 2006;140:1384–95. [PubMed: 16691619]
40. Ye W, Shimamura K, Rubenstein JLR, Hynes MA, Rosenthal A. FGF and Shh Signals Control Dopaminergic and Serotonergic Cell Fate in the Anterior Neural Plate. Cell 1998;93:755–66. [PubMed: 9630220]
41. Guo S, Brush J, Teraoka H, et al. Development of noradrenergic neurons in the zebrafish hindbrain requires BMP, FGF8, and the homeodomain protein soulless/Phox2a. Neuron 1999;24:555–66. [PubMed: 10595509]
42. Nechiporuk A, Linbo T, Poss KD, Raible DW. Specification of epibranchial placodes in zebrafish. Development 2007;134:611–23. [PubMed: 17215310]
43. Kawauchi S, Shou J, Santos R, et al. Fgf8 expression defines a morphogenetic center required for olfactory neurogenesis and nasal cavity development in the mouse. Development 2005;132:5211–23. [PubMed: 16267092]
44. Wang C, Xia C, Bian W, et al. Cell aggregation-induced FGF8 elevation is essential for P19 cell neural differentiation. Mol Biol Cell 2006;17:3075–84. [PubMed: 16641368]
45. Reimers D, López-Toledano MA, Mason I, et al. Developmental expression of fibroblast growth factor (FGF) receptors in neural stem cell progeny. Modulation of neuronal and glial lineages by basic FGF treatment. Neurol Res 2001;23:612–21. [PubMed: 11547930]
46. Nissen RM, Yan J, Amsterdam A, Hopkins N, Burgess S. Zebrafish foxi one modulates cellular responses to Fgf signaling required for the integrity of ear and jaw patterning. Development 2003;130:2543–2554. [PubMed: 12702667]
47. Marsh SK, Bansal GS, Zammit C, et al. Increased expression of fibroblast growth factor 8 in human breast cancer. Oncogene 1999;18:1053–60. [PubMed: 10023681]

48. Dorkin TJ, Robinson MC, Marsh C, Bjartell A, Neal DE, Leung HY. FGF8 over-expression in prostate cancer is associated with decreased patient survival and persists in androgen independent disease. Oncogene 1999;18:2755–61. [PubMed: 10348350]

49. Mattila MM, Harkonen PL. Role of fibroblast growth factor 8 in growth and progression of hormonal cancer. Cytokine Growth Factor Rev 2007;18:257–266. [PubMed: 17512240]

50. Hunter DJ, Kraft P, Jacobs KB, et al. A genome-wide association study identifies alleles in FGFR2 associated with risk of sporadic postmenopausal breast cancer. Nat Genet 2007;39:870–4. [PubMed: 17529973]

51. Huijts PE, Vreeswijk MP, Kroeze-Jansema KH, et al. Clinical correlates of low-risk variants in FGFR2, TNRC9, MAP3K1, LSP1 and 8q24 in a Dutch cohort of incident breast cancer cases. Breast Cancer Res 2007;9:R78. [PubMed: 17997823]

52. Zhong C, Saribekyan G, Liao CP, Cohen MB, Roy-Burman P. Cooperation between FGF8b overexpression and PTEN deficiency in prostate tumorigenesis. Cancer Res 2006;66:2188–94. [PubMed: 16489020]

53. Moore JL, Aros M, Steudel KG, Cheng KC. Fixation and decalcification of adult zebrafish for histological, immunocytochemical, and genotypic analysis. BioTechniques 2002;32:300–4. [PubMed: 11848406]

54. Amsterdam A, Hopkins N. Retroviral-mediated insertional mutagenesis in zebrafish. Methods Cell Biol 2004;77:3–30. [PubMed: 15602903]

55. Danielian PS, Bender Kim CF, Caron AM, Vasile E, Bronson RT, Lees JA. E2f4 is required for normal development of the airway epithelium. Dev Biol 2007;305:564–76. [PubMed: 17383628]

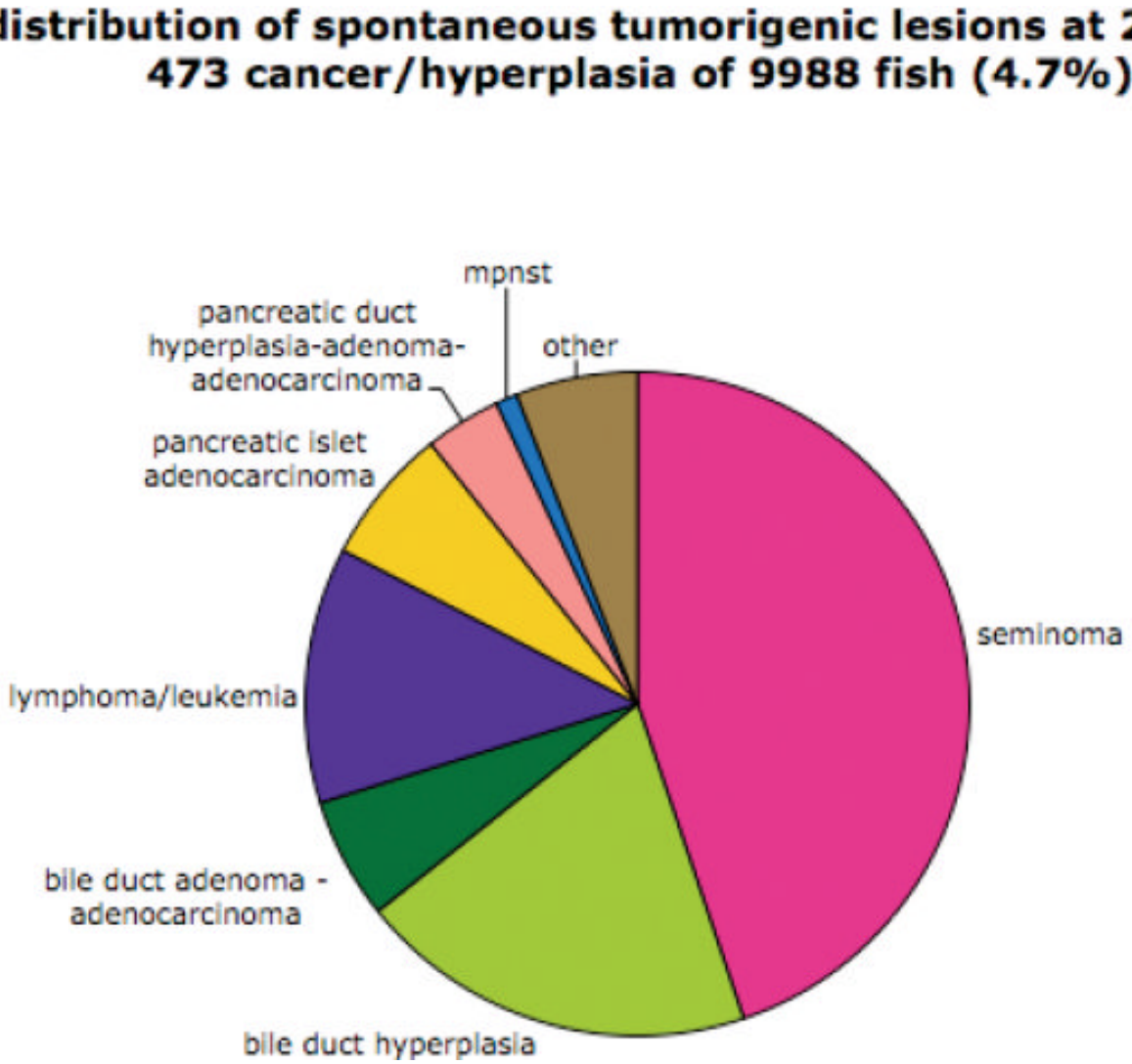

Figure 1.
Distibution of types of tumorigenic lesions in the background population.

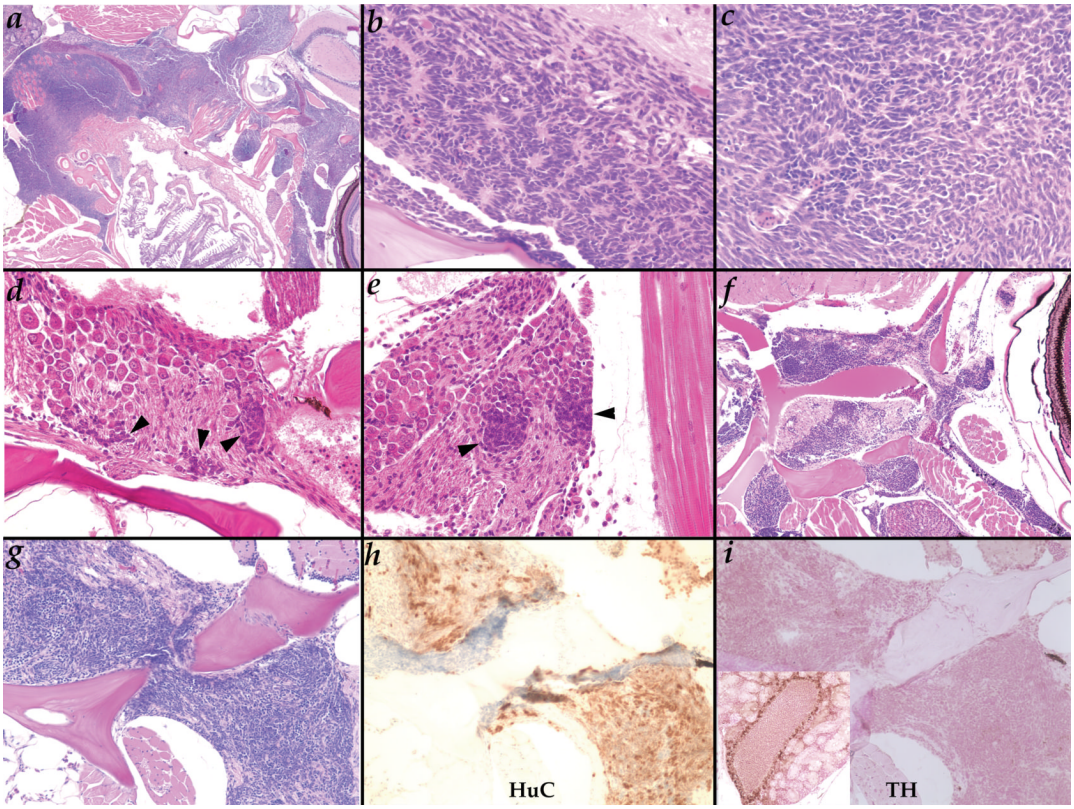

Figure 2.

Neuroblastoma-like tumors in *Hag* heterozygotes at two years of age. **A.** (40X) a very advanced tumor fills most of the head space between the esophagus and the skull and invades the body wall musculature; **B-C.** (400X) rosette arrangement of cells is occasionally observed in tumors (B) but more commonly cellular arrangement is more variable (C); **D-E.** (400X) very small neoplasias (black arrowheads) observed in the ganglia within the skull below the midbrain (D) or posterior of the ear (E); **F.** (100X) this tumor can be seen growing along the nerve running behind the eye as well as another below the skull; **G-I**. (200X) H&E (G), anti-HuC (H), and anti-TH (**I)** of the same tumor; inset in I shows TH staining of adrenal cells in the kidney on the same slide as a positive control for the antibody.

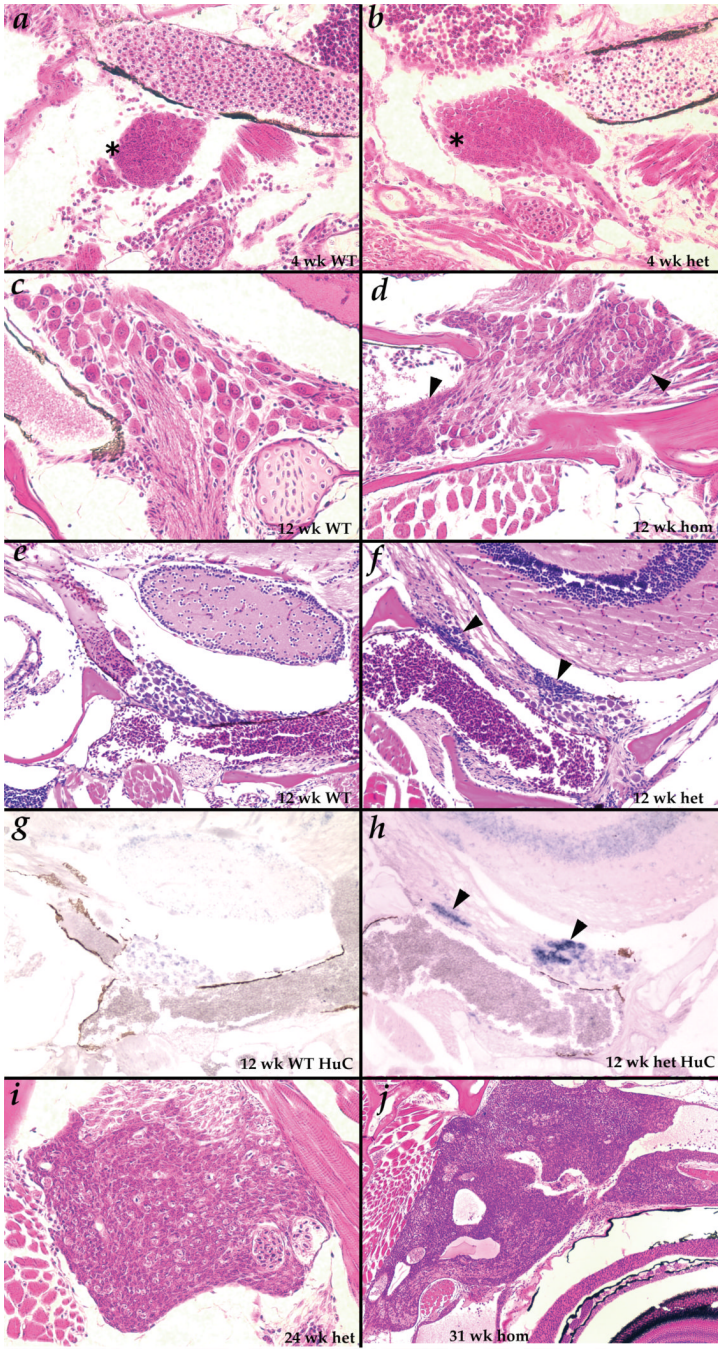

Figure 3.

Tumors begin as inappropriate maintenance of a normal developmental stage of putative neural precursors. **A-B.** (400X) at 4 weeks small cells resembling the tumor cells (asterisks) are seen in cranial ganglia of both wild type (A) and *Hag* (B) fish; **C-D.** (400X) at 12 weeks, only fully developed ganglion cells are observed in wild type fish (C), but the small precursor-like cells (black arrowheads) are still observed in most *Hag* mutants (D). **E-H.** (200X) the small cells seen uniquely in *Hag* mutants (black arrowheads) at 12 weeks (F) stain strongly for HuC mRNA by in situ hybridization (H); ganglion cells in wild type (E) and *Hag* mutants (F) stain weakly for HuC (G,H); **I.** (400X) tumor beginning to spread over entire ganglia in 24 week *Hag*

heterozygote; **J.** (100X) tumor in 31 week homozygote growing within the skull and along nerves behind and above the eye.

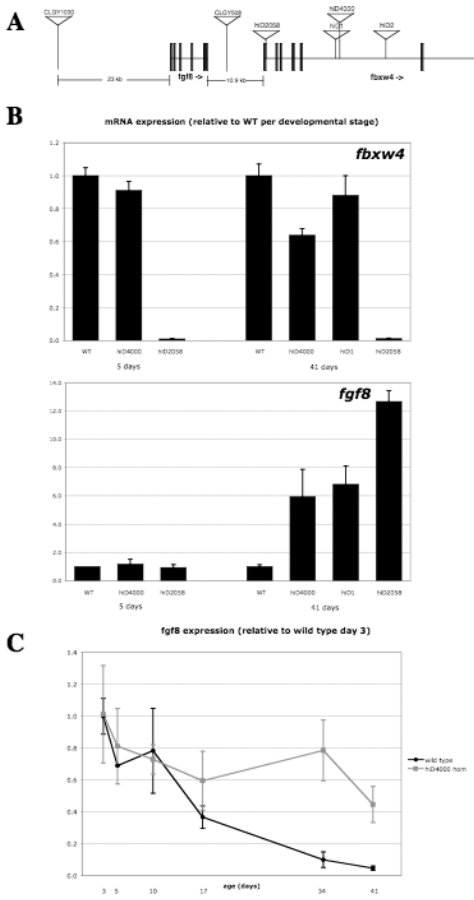

Figure 4.

Hag mutations are insertions in the *fbxw4* gene but affect expression of the neighboring *fgf8* gene. **A.** Location of the mutagenic insertions in *Hag* mutants. hiD2058 is precisely at the splice donor of exon 1 of *fbxw4*; the other three insertions are in the 24 kb fifth intron. Enhancer trap insertions CLGY1030 and CLGY508 are in intergenic sequence upstream and downstream of *fgf8*, respectively. **B.** *fbxw4* and *fgf8* mRNA measured in whole fish by real-time RT-PCR in wild type and homozygotes of multiple *Hag* alleles at 5 and 41 days. Units are normalized to wild type sample of each developmental age. **C.** *fgf8* mRNA measured in whole fish by real-time RT-PCR in wild type and hiD4000 homozygotes from 3 to 41 days. Units are normalized to the 3 day wild type sample. For B and C, error bars show the standard deviation of 2−3 technical replicates.

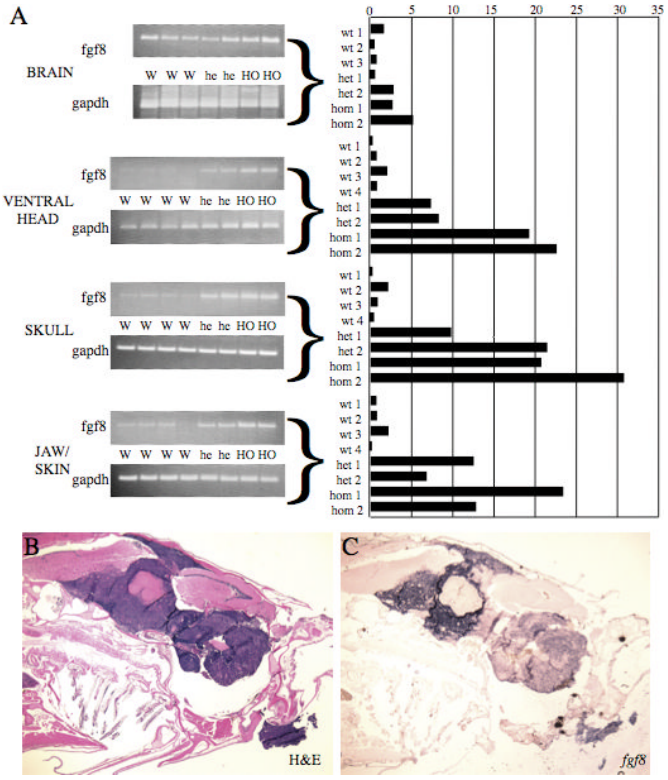

Figure 5.

Hag mutants overexpress *fgf8* in the head region of young adults and in tumors **A.** *fgf8* mRNA in multiple parts of the head of 3 month old wild type, hiD2058 heterozygote and hiD2058 homozygote fish were measured by real-time and semi-quantitative RT-PCR; *gapdh* was used as a normalization control. Samples were isolated from three (brain) or four wild type fish and two each Hag^{hi2058} heterozygotes and homozygotes. Ethidium bromide stained gels from semi-quantitative RT-PCR are shown on the left; quantification of the real-time PCR is shown on the right. Quantification is normalized within the dataset for each tissue to the average wild type sample of that tissue; error bars show the standard deviation of three technical replicates. **B-C.** (20X) H&E (B) and *fgf8* in situ hybridization (C) on a very advanced tumor in a 2 year old hiD2058 homozygote.

Table 1

Incidence of neuroblastoma in 2 year old *Hag* heterozygotes and their wild type siblings

Allele		Wild type	Heterozygote
hiD1	Total tumors	0/34	16/34 (47%)
	Small neoplasias	0/34	7/34 (21%)
	Advanced tumors	0/34	9/34 (26%)
hiD2	Total tumors	0/56	19/77 (25%)
	Small neoplasias	0/56	19/77 (25%)
	Advanced tumors	0/56	0/77
hiD2058	Total tumors	0/39	17/38 (45%)
	Small neoplasias	0/39	13/38 (34%)
	Advanced tumors	0/39	4/38 (11%)
hiD4000	Total tumors	0/24	18/59 (30%)
	Small neoplasias	0/24	9/59 (15%)
	Advanced tumors	0/24	9/59 (15%)

Table 2

Incidence of neural neoplasias and advanced neuroblastoma in *Hag* heterozygotes, homozygotes and wild type siblings over time

Allele	Age (weeks)		Wild types	Heterozygotes	Homozygotes
hiD4000	12	Small neoplasias	0/17	28/30 (93%)	17/20 (85%)
		Advanced tumors	0/17	0/30	0/20
		Dead*	0/17	0/30	0/20
	24	Small neoplasias	0/10	20/28 (71%)	7/9 (78%)
		Advanced tumors	0/10	1/28 (4%)	0/9
		Dead*	0/10	0/28	4/13 (31%)
	31	Small neoplasias	0/16	18/28 (64%)	0/2
		Advanced tumors	0/16	0/28	1/2 (50%)
		Dead*	0/16	0/28	6/8 (75%)
	39	Small neoplasias	N.D.	6/14 (43%)	3/10 (30%)
		Advanced tumors	N.D.	2/14 (14%)	4/10 (40%)
		Dead*	N.D.	0/14	7/17 (41%)
hiD1	17	Small neoplasias	0/10	22/26 (85%)	9/11 (82%)
		Advanced tumors	0/10	0/26	0/11
		Dead*	N.D.	N.D.	N.D.
	24	Small neoplasias	0/21	37/52 (71%)	3/13 (38%)
		Advanced tumors	0/21	6/52 (11%)	4/13 (31%)
		Dead*	N.D.	N.D.	N.D.
	34	Small neoplasias	N.D.	3/10 (30%)	3/7 (43%)
		Advanced tumors	N.D.	3/10 (30%)	2/7 (29%)
		Dead*	N.D.	0/10	2/7 (29%)
hiD2058	17	Small neoplasias	0/16	14/17 (82%)	9/11 (82%)
		Advanced tumors	0/16	0/17	0/11
		Dead*	N.D.	N.D.	N.D.
	24	Small neoplasias	0/15	29/37 (78%)	8/11 (73%)
		Advanced tumors	0/15	0/37	2/11 (18%)
		Dead*	N.D.	N.D.	N.D.
	34	Small neoplasias	0/6	5/11 (45%)	4/14 (29%)

Allele	Age (weeks)		Wild types	Heterozygotes	Homozygotes
		Advanced tumors	0/6	4/11 (36%)	6/14 (43%)
		Dead*	0/6	0/11	4/18 (22%)
hiD2	24	Small neoplasias	0/12	33/38 (87%)	11/17 (64%)
		Advanced tumors	0/12	0/38	1/17 (6%)
		Dead*	N.D.	N.D.	N.D.

*these fish died from wasting, presumably subsequent to severe esophageal/gut inflammation, not from tumors. N.D., not determined.